tvst

https://doi.org/10.1167/tvst.8.6.14

Article

Observational Clinical Studies of Human Lens Transparency Using the Vision Index Pen

Azin Abazari[1], Harbans S. Dhadwal[2], and John Wittpenn[3]

[1] Department of Ophthalmology, SUNY Stony Brook, Stony Brook, NY, USA
[2] Integrated Fiber Optic Systems, Inc, Stony Brook, NY, USA
[3] Ophthalmic Consultants of Long Island, East Setauket, NY, USA

Correspondence: Azin Abazari, Stony Brook University Health Science Center, Department of Ophthalmology, 101 Nicolls Rd, Stony Brook, NY 11794, USA. e-mail: azin.abazari@stonybrookmedicine.edu

Received: 16 April 2019
Accepted: 27 September 2019
Published: 15 November 2019

Keywords: cataract; presbyopia; accommodation; opacification; lens crystallins; dynamic light scattering

Citation: Abazari A, Dhadwal HS, Wittpenn J. Observational clinical studies of human lens transparency using the Vision Index Pen. Trans Vis Sci Tech. 2019;8(6):14, https://doi.org/10.1167/tvst.8.6.14

Purpose: Preventing or delaying the onset of presbyopia and cataract formation remains a challenge. The goal of this study was to establish the utility of the Vision Index Pen (VIP), designed to measure in vivo dynamic light scattering (DLS) from the crystalline lens, in the detection of early cataract or loss of accommodation and to show reproducibility through trials at two independent sites. The gradual loss of transparency of the lens was characterized by the lens crystallin aggregation index (LCX) derived from measured DLS data.

Methods: Volunteers in different age groups participated in two independently operated observational clinical studies. All subjects underwent a detailed eye exam and VIP measurement of the intensity correlation of the backscattered light from the lens.

Results: LCX values extracted from DLS data show strong correlation with the aging lens, ranging from 20 at the age of 20 years to over 150 at 60 years. Quantitatively significant changes in the LCX value occur from 35 years to 55 years. LCX values were found to correlate with the loss of accommodation (correlation of -0.563 with $P < 0.001$) and with published data regarding the change in relative lens resistance with age.

Conclusions: Results from two independent observational clinical trials have confirmed the repeatability and reproducibility of the VIP diagnostic device as a viable clinical tool for tracking localized macromolecular changes taking place in the aging lens. Detection of early changes in the crystalline lens can be useful in developing patient-specific prediction models, which can be used to screen patients who may benefit from early therapeutic interventions for delaying the onset of presbyopia and cataract growth.

Translational Relevance: The VIP diagnostic device provides in vivo access to the human lens, enabling characterization of the unfolding and decomposition of long-lived macromolecules.

Introduction

Cataract is a leading cause of treatable vision loss globally.[1] Patients with cataract can experience decreased visual acuity, loss of contrast sensitivity, glare, and altered color perception. Visually significant cataract not only lowers health-related quality of life due to its effects on vision but also can cause functional and psychological disability.[2,3] With the aging population, an increase in the number of individuals with visually significant cataract and a rise in the financial burden of cataract surgery are expected.[4,5] Therefore, the development of alternatives to cataract surgery, treatments to prevent cataract formation in high-risk populations, and progression of early-stage cataract are of substantial value.

It has been shown in animal studies that early intervention is needed to slow the aging process of the lens and reverse cataract formation.[6,7] Currently, slit lamp biomicrosopy, Scheimpflug imaging, and optical

coherence tomography (OCT) are used to detect cataract in the clinical stage or provide high-resolution images of the lens. Nevertheless, cataract formation can potentially be detected much earlier at the preclinical level by using dynamic light scattering (DLS), which has been used over the past three decades to study cataract.[8–15] However, designing a DLS device to provide reliable and repeatable measurements of light scatter from the lens and defining a valuable index to detect and grade preclinical cataractous changes in the lens remain challenging. In this study, the clinical utility of the VIP diagnostic device to measure in vivo DLS from the lens and to detect early cataract or loss of accommodation is evaluated.

Despite the recent abundance of in vivo DLS clinical data from human lenses, the development of a viable routine instrument has alluded researchers. This has been primarily due to the lack of reliable and robust analytical methods for interpreting the in vivo DLS data. Although the complexity of the backward scattered light from the lens is generally appreciated, DLS data continue to be interpreted as arising from an equivalent model based on Brownian diffusion in a low concentration regime.[16,17] In previous studies, the analysis of measured data was further compromised by the insistence on extracting far too much information than is typically available from in vivo DLS clinical data. Additional data inversion difficulties arise due to the involuntary blinking and reflex action of the eye during clinical measurement. The weak backward scattered signals originate from the crystallins contained within each of the fiber cells making up the lens. These fiber cells, particularly in the nuclear region of the lens, have shed the nucleus, organelles, and other scattering material and can be viewed as liquid crystals at very high protein concentrations (300 mg/mL), comprising α-, β-, and γ-crystallins.[18–23] Of these, α-crystallin is the largest and likely the major component of the scattered signal. These small macromolecules, even in the high concentrations, are responsible for the time-varying signals measured with DLS. These signals have detectable temporal features in the nanosecond time scales. No other biochemical process in the human body has these rapid time scales. Over the normal aging process, in vitro studies have shown that the γ-crystallins, in the presence of the unfolding of α-crystallins,[24] aggregate into larger macromolecules.[22] Both the aggregation and unfolding of proteins lead to an increase of the size of the macromolecules, causing the macromolecules to slow down. DLS techniques can detect these temporal changes and provide a window into the underlying macromolecular dynamics. The VIP device extracts a dominant temporal signature from the measured correlation function and associates its value with the localized transparency of the lens, expressed as lens crystallin aggregation index (LCX).

In a recent review on long-lived proteins, Truscott and colleagues[18,20] noted that due to significant differences in the human lens compared with those of nonprimates, understanding of the underlying macromolecular changes associated with human age-related conditions, such as presbyopia and cataract, requires in vivo investigations. Characterizing the unfolding and decomposition of long-lived macromolecules is key to understanding these disorders. We designed the VIP device to estimate the aggregation index of lens proteins and detect cataract at the subclinical level. The VIP diagnostic device can be a catalyst in promoting experimental research into the etiology of cataract and presbyopia in the aging human lens by providing a continuous stream of in vivo data acquired at different clinical sites.

Materials and Methods

This is an observational clinical study operated at two independent sites. Site 1 had a patient population of 86 with 35 males and 45 females. Site 2 had a patient population of 73 with 33 males and 40 females. Sex data were not recorded for six patients in site 1. Patients were divided by age into five groups. Table 1 shows the subject population in each of the five target age groups for the two clinical sites.

Measurement accuracy and repeatability of the VIP device were evaluated using a dual-walled glass cell mounted on the slit lamp (see Fig. 1). The inner 3-mm cylindrical cell, containing a scattering solution of polystyrene spheres, represents the nuclear region of the lens. The 12-mm outer cylindrical cell, filled with filtered water, represents the nonscattering space between the anterior surface of the lens and the posterior surface of the cornea. This arrangement provides replication of the multiple reflecting interfaces that are present in the eye, creating a more realistic but fixed system for training and testing. The diameter of certified traceable polystyrene spheres, at a concentration of 100 mg/mL, was measured within 2% accuracy (PLS22; Bangs Laboratory, Fishers, IN). The VIP device measures a scattering volume of 0.225 nL.

The two independent studies followed the tenets of

Table 1. Trial Population and Age Distribution at the Two Clinical Sites

	Site 1						Site 2					
Study Population	AG1	AG2	AG3	AG4	AG5	Total	AG1	AG2	AG3	AG4	AG5	Total
Age range (years)	20–29	30–39	40–49	50–59	>60		20–29	30–39	40–49	50–59	>60	
Population (*n*)	17	11	11	16	31	86	20	17	6	16	14	73

AG, age group.

Declaration of Helsinki. One study protocol was approved by the Committee on Research Involving Human Subjects at the State University of New York at Stony Brook, whereas the second study was approved by the Sterling Institutional Review Board (Atlanta, GA). Informed consent was obtained from all subjects after explanation of the nature and possible consequences of the study. Subjects with uveitis, corneal disorders, previous cataract surgery, or at risk for pupillary dilation (narrow anatomical angle or history of allergic reaction to one of the dilating drops) were excluded. All subjects underwent a detailed eye exam, including measurement of best-corrected distance and near visual acuity, amplitude of accommodation, and slit lamp examination for grading of cataract. Best-corrected Snellen visual acuity was recorded and then converted to logarithm of the minimum angle of resolution (LogMar) visual acuity. The left eye of each subject was chosen for the study. To measure the amplitude of accommodation, phoropter was used to refract the subject and achieve the best-corrected distance vision. The right eye was then occluded. In a well-illuminated room, the subject's left near vision was checked at 66 cm after adding +1.5 diopter over the distance correction. Then, the subject was directed to focus one line above the line, which they could comfortably read with this correction. The near card was moved smoothly toward the subject until they could not identify the letters on that line anymore. The distance of the near card from the phoropter was recorded in centimeters. The measurement was repeated three times, and the average reading was converted to diopter. A total of 1.5 diopter was subtracted from this measurement to record the average amplitude of accommodation, with a measurement error smaller than 0.5.

After the pupil was adequately dilated, a single ophthalmologist investigator in each center graded the lens opacity from clear to trace; 1+, 2+, or 3+ for nuclear sclerosis; and mild, moderate, and significant for cortical and posterior subcapsular cataract based on the slit lamp exam. The repeatability of clinical grading for each examiner was over 90%. The subject was then positioned at the slit lamp mounted with the VIP device (Fig. 2) and instructed to fixate on the

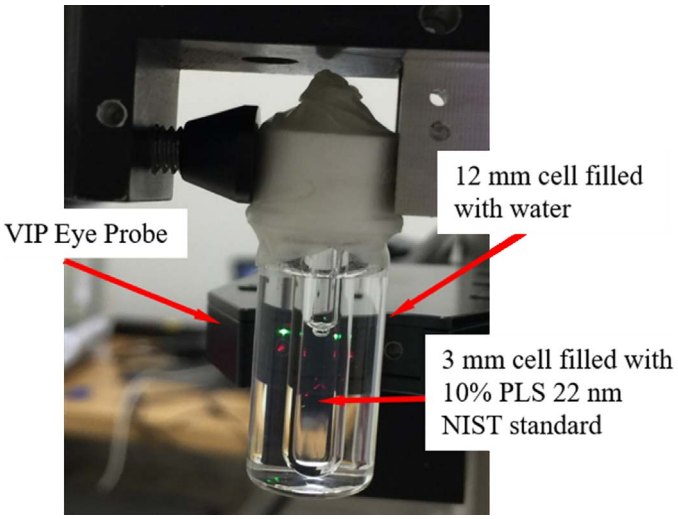

Figure 1. A dual cell model for the human lens used for characterizing the repeatability of the VIP device. A 3-mm cylindrical glass cell, containing a National Institute of Standards and Technology traceable sample of 10% by weight polystyrene spheres, was immersed in a 12-mm cell containing filtered water.

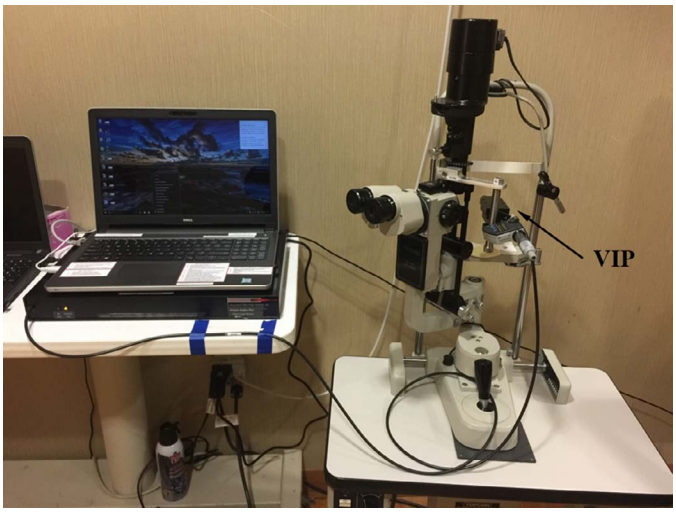

Figure 2. Photograph of the VIP system in the clinical setting. The VIP head is mounted onto a standard slit lamp.

white target light in the center of the fiber optic probe head. For each measurement, the examiner positioned the cross-over point of two laser beams in the center of the lens, 5 mm from the surface of the cornea measured by means of a digital micrometer. During measurement, one of the laser beams was turned off and the backscattered laser light from the cross-over point was measured over 10 seconds. Eye safe laser exposure was set according to ANSI standard[25]. The subject was asked to avoid blinking during each measurement. The measurement was repeated five times. Intensity correlation of the back scattered light was processed to recover a localized LCX value, corresponding to the degree of aggregation of the crystallins in the nuclear region of the lens. Backward scattered laser light, typically from 100 fiber cells, is transported back to the electronics modules by using single-mode optical fibers threaded through a connecting tether assembly (Fig. 2). At the distal end, the laser signal is divided into two equal components by using a 1×2 single-mode fiber optic power splitter. Weakly scattered signals are detected by avalanche-photodiode-based single-photon counting modules. The two photon-electron data streams are processed in real-time to obtain a cross-correlation of the backward scattered laser light over a time scale from 12.5 ns to 1 second.

Some of the popular algorithms for inverting the measured correlation are described in several classical textbooks on the subject.[16] Although most inversion techniques are based on Brownian diffusion (low concentration regime), there are some that are developed for gel-like systems[26] typical of the high concentration scattering systems, such as the lens. Some arguments have been made to support the use of these models for inverting in vivo correlation data from the lens. Of these, the most promising, the stretched exponential model,[27] did not yield consistent inversion of the in vivo-measured correlation data collected from the lens. Other non-Brownian motion models have been proposed for similar in vitro systems but have not been successfully applied to in vivo measurements from the eye.[28]

In addition to the above modeling concerns, data inversion algorithms require very accurate estimates of the baseline, typically within 0.3%. The baseline corresponds to the flat, uncorrelated region at large delay time increments, that is, proportional to the square of average value of the scattered signal. As can be appreciated, eye movement and reflex action can lead to large abrupt changes in the average scattered signal. Blinking causes momentary occlusion (zero signal), whereas reflex action can dramatically cause an increase in the average scattered signal. Both of these involuntary patient responses have a deleterious effect on the baseline estimates and prevent meaningful interpretation of the correlation data.

The above unavoidable deleterious effects limit the amount of information that can be extracted from the measured data. In view of these difficulties, a single parameter corresponding to the fastest characteristic time of the macromolecular motion was extracted from the measured correlation data by using nonlinear least squares curve fitting based on a modified second-order cumulant model.[29] The measured characteristic time is transformed to the LCX value, which is proportional to the size of the largest crystallin in the localized measurement volume. The LCX value, which is device and operator independent, can be used to track changes in the localized aggregation of the crystallin within the lens fiber cells.

Statistical Analysis

Five measurements for each patient were attempted, and for the patient data to be included in the analysis, at least three good measurements per patient were required. Data analysis, including nonlinear least squares curve fitting based on the Levenberg method, was performed using MATLAB 2018b (MathWorks, Boston, MA). Additional statistical analysis was performed using SPSS version 25.0 (SPSS Inc., Chicago, IL). A P value less than 0.05 was considered statistically significant. The Pearson or Spearman correlation analysis was performed to evaluate the relationship between parameters depending on the normality of the parameters.

Results

In our study, as expected, the amplitude of accommodation declined with aging. Figure 3 shows the measured amplitude of accommodation at the first site (diamond symbols). Based on three measurements, the error was calculated to be less than 0.5 diopter. The solid line is based on measurements from over 1000 patients that were reported by Duane.[30] The measured data fall within the expected lower and upper limits of accommodation as a function of age.

In our study, LCX value increased with age. Figure 4 shows the variation of the measured LCX values in site 2 for patients in the first age group from 20 years to 29 years old and for patients in the last age group (>60 years). The error bars are based on the standard

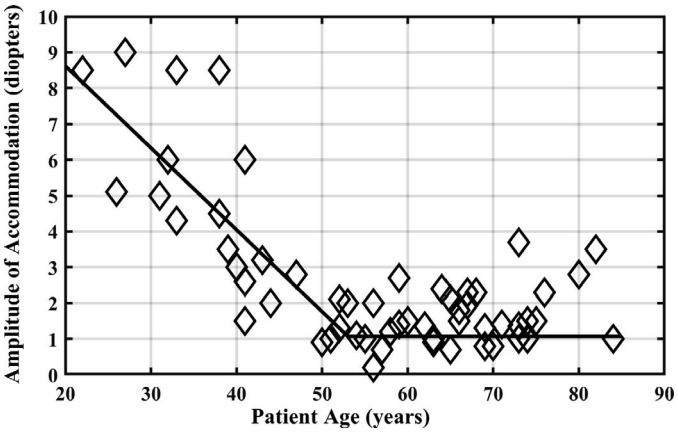

Figure 3. Amplitude of accommodation from patient data at site 1. *Diamond symbols* are measured data, and the *solid line* is a linear fit described by Duane.[30]

deviation of 3 to 5 measurements for each patient. The average value of LCX for the first age group is 23.4 ± 6.0, and for the last age group it is 150.1 ± 70.4. Patients with fewer than three acceptable measurements were excluded from the summary plots.

Figure 5 shows a plot of the average LCX value for all patients measured at the first site. The vertical dotted line indicates the resolution limit of clinical examination, that is, all patients below the age of 50 years were classified to have clear lenses based on slit lamp exam. On the right side of the vertical bar, the plot is annotated with clinical classification of the progressing cataract for few selective patients. Similarly, the results of the VIP measurements at the second site are summarized in Figure 6.

As expected, LCX increased with decreasing amplitude of accommodation. Figure 7 shows a scatter plot of the logarithmically scaled LCX values and the corresponding amplitude of accommodation from data at site 1. The data show a strong negative Spearman correlation of −0.563 with $P < 0.001$. Accommodation measurements from the second site were compromised by an unknown systematic error and have been excluded here. Although the data from site 1 showed good correlation between accommodation and LCX, it should be noted that the LCX characterizes lens properties at the molecular level, whereas the accommodation is representative of macroscopic changes, corresponding to lens equatorial diameter and axial thickness.

Figure 8 shows a comparison of the LCX values obtained from the two independent sites. The unscaled values of LCX, obtained with two independent VIP systems, which were operated by independent ophthalmologists, have not been scaled in any way. Results from the two the clinical sites, grouped by the five age groups, are summarized in Table 2.

Discussion

The LCX values obtained at both sites and summarized in Figure 8 confirm the repeatability and reproducibility of the VIP as an ophthalmic diagnostic device to identify early cataractous changes in the lens, long before they are clinically observable. As expected, the spread in the LCX values for the first two age groups (20 to 39 years) is small compared with the spread over the remaining age groups. Figure 9 shows a plot of LCX data over age bracket 35 to 55 years. Measurable changes in the LCX over this age group are critical for the development of therapeutic agents for delaying the onset of presbyopia and cataract.

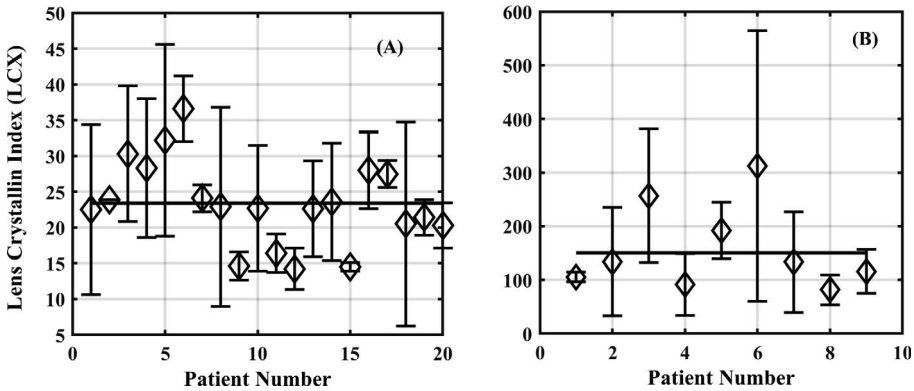

Figure 4. A summary of the LCX values for volunteers in the first age group (20 to 29 years) (*left* graph) and for last age group (older than 60) (*right* graph). In the first age group, the LCX has a mean value of 23.4 with a standard deviation of 6.0. In the last age group, the LCX has a mean value of 150.1 with a standard deviation of 70.4.

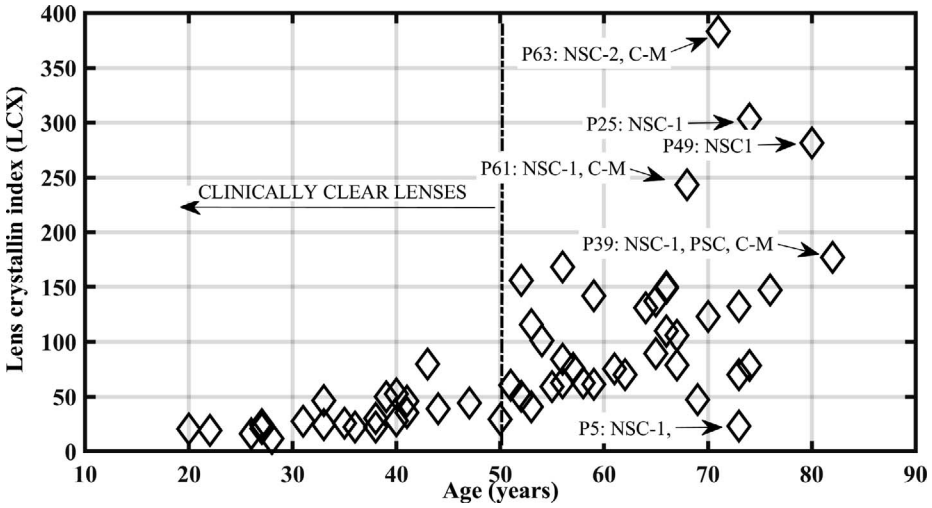

Figure 5. A summary of the VIP-derived LCX values at site 1. The *vertical dotted line* indicates the lower limit, below which clinical examination is not effective for characterizing the lens. NSC, nuclear sclerotic cataract; C, cortical cataract; PSC, posterior subcapsular cataract; M, moderate.

The question is always asked of a new diagnostic device as to how it compares with the existing devices. However, it should be noted that comparing clinical examination grading of lenses with the LCX values presents a challenging problem as the former makes observations at the macroscopic scale, whereas the latter is probing at the macromolecular level, with a dynamic range spanning over three orders. In view of these differences, a more meaningful metric for comparison here is to establish an age range over which changes in the lens transparency can be reliably assessed. Quantitative comparison is possible by comparing the dynamic range of each method for characterizing lens clarity (or transparency) averaged over each age group studied here. For each age group, the percentage of lenses classified as clear by each method was extracted. The results are plotted in Figure 10 site 1 (top panel) and site 2 (bottom panel), respectively. For the VIP device, an LCX value smaller than 30 is attributed to clear, noncataract lenses. From the data presented, it can be ascertained that the VIP device provides a reproducible, quantitative measurement throughout the aging lens from 20 years onward, while clinical grading methods are

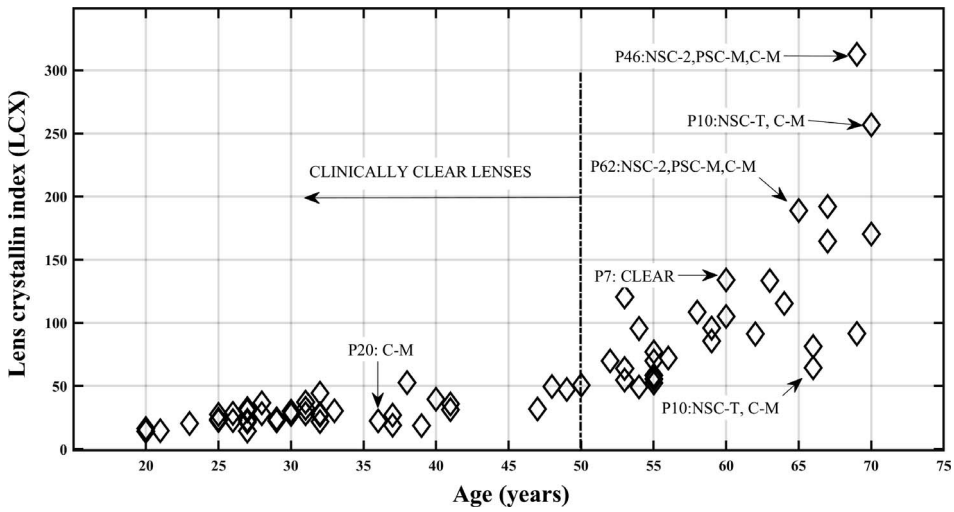

Figure 6. A summary of the VIP-derived LCX value based on age at site 2. The *vertical dotted line* indicates the lower limit, below which clinical examination is not effective for characterizing the lens. NSC, nuclear sclerotic cataract; C, cortical cataract; PSC, posterior subcapsular cataract; M, moderate; T, trace.

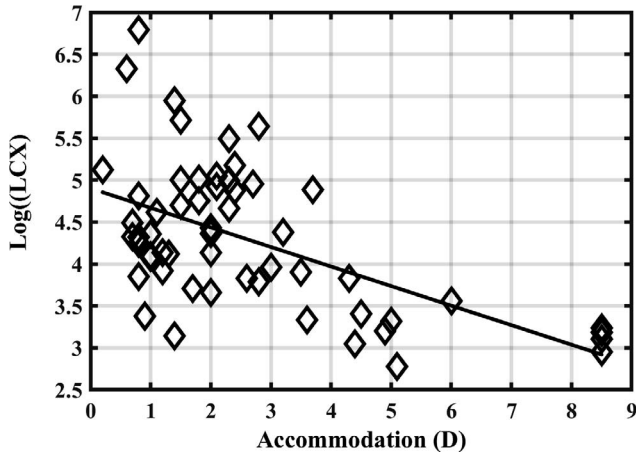

Figure 7. Correlation between the VIP-derived LCX value and the measured accommodation for volunteer data from site 1. The correlation value is −0.563 with $P < 0.001$.

Figure 8. Correlation between the VIP-derived LCX values and age from the two independently run trials at the two sites. *Squares* and *diamonds* are data from site 1 and site 2, respectively.

useful, nominally after the age of 45 years. The same can be said of most imaging methods, as their detection limit is also measured at the macroscopic scale, with an arbitrary number of grey scale levels for classification. Such methods are primarily used for the management of clinically observable cataracts. However, it should be noted that other objective technologies have emerged to extend the limits of current methods for the grading of the lens aging, from presbyopia to cataract. iTrace (visual function analyzer) characterizes the aberrated lens system with a dysfunctional lens index,[31,32] which is derived by ray-tracing techniques. The Optical Quality Analysis Device II quantitates the imaging capability of young lenses through the measured modulation transfer function and the contrast sensitivity function.[33,34]

Table 2. Summary of Measured Data From Both Clinical Sites

	Site 1					Site 2				
Measured Item	AG1 20–29	AG2 30–39	AG3 40–49	AG4 50–59	AG5 >60	AG1 20–29	AG2 30–39	AG3 40–49	AG4 50–59	AG5 >60
Group population (*n*)	8	9	7	15	24	20	17	6	16	14
Number of patients with clear lens based on clinical exam	8	9	7	7	2	20	17	6	8	1
VIP (LCX, <30)	7	5	0	0	1	17	9	0	0	0
% Clear (clinical exam)	100.0	100.0	100.0	46.7	8.3	100.0	100.0	100.0	50.0	7.1
% of patients with LCX <30	87.5	55.6	0.0	0.0	4.2	85.0	52.9	0.0	0.0	0.0
LCX										
Group mean	19.4	25.3	36.3	84.6	189.7	23.0	50.1	39.2	73.7	150.1
Group SD	6.0	3.2	16.6	42.7	42.7	6.0	8.7	8.2	21.8	70.4
AoA										
Group mean	6.9	6.1	3.5	1.4	1.5	2.4	1.7	1.9	1.9	1.4
Group SD	4.9	2.1	1.5	0.6	0.7	2.4	1.4	0.9	0.9	0.5
VA (logMar)										
Group mean	0.070	0.0	0.010	0.018	0.071	−0.040	−0.034	−0.020	−0.018	0.029
Group SD	0.150	0.0	0.050	0.050	0.100	0.084	0.076	0.117	0.126	0.132

VA, visual acuity; AoA, amplitude of accommodation.

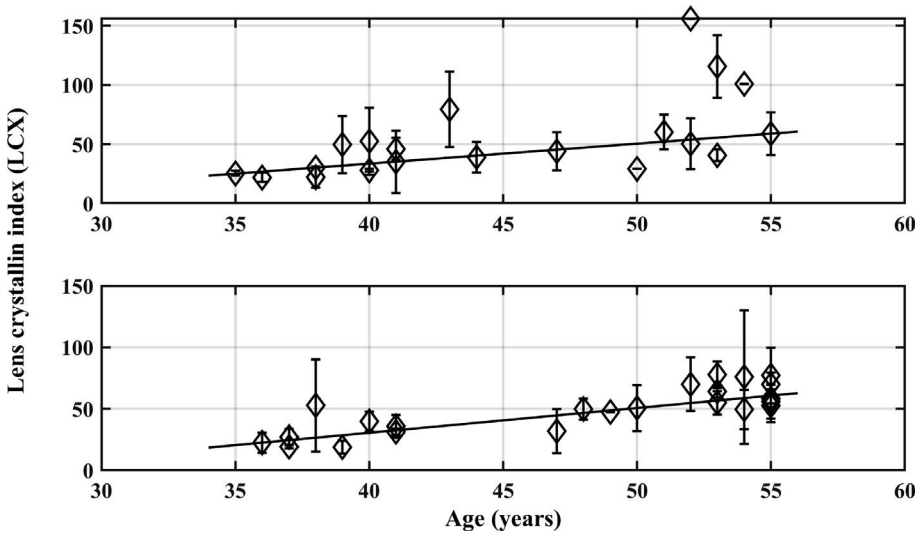

Figure 9. Correlation between the VIP-derived LCX values from the two independently run trials at the two sites. Data from site 1 (*top* panel) and site 2 (*bottom* panel), respectively. A linear fit for the two sites is described by the equations $LCX = 1.69x(age - 20.1)$, with a r^2 value of 0.886, and for site 2 is $LCX = 2.0x(age - 24.9)$, with a r^2 value of 0.630.

Even though the data collected here is not over the life of the same lens, it is still meaningful to explore some additional trends and properties that have been observed at the macromolecular scale. Although the debate on the origins of presbyopia is still ongoing, as discussed by Truscott[18] and Koretz,[22] it is generally accepted that presbyopia and cataract progression in the lens is accompanied by an increase in the relative lens resistance (RLR), or otherwise referred to as lens stiffness. Glasser and Campbell[35] have made extensive measurements of RLR from excised human lenses and found that RLR increases after the onset of presbyopia. Figures 11 and 12 show the results (solid line) of a nonlinear least squares curve fit to the LCX data by using the RLR model. The fit parameters for site 1 are $LCX = 15.8 + 3.0 \times 10^{-3}(age)^3$, with an r^2 value of 0.966, and for site 2 $LCX = 15.5 + 3.8 \times 10^{-3}(age)^3$, with an r^2 value of 0.986. The dash-dot lines in Figures 11 and 12 show the result of a nonlinear least squares curve fit to the LCX measured data by using an exponential growth model. The exponential growth model for site 1 is described as

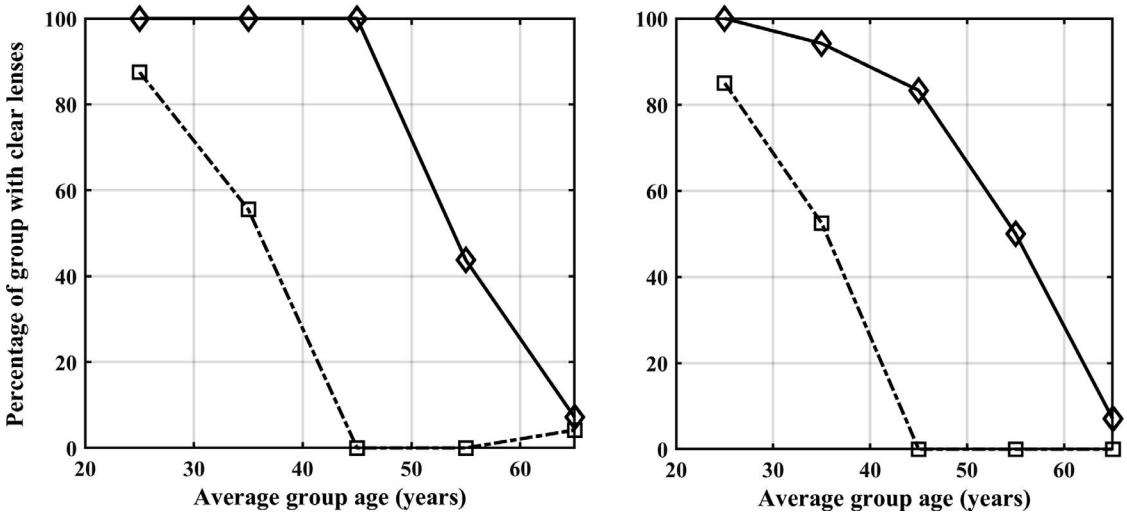

Figure 10. Comparison of VIP (*dash-dot*) and clinical grading (*solid line*) for site 1 (*left* graph) and site 2 (*right* graph). Each *point* represents the average value for each of the age groups, and the *points* are centered at the mid-point of each respective age group. The figure shows that clinical examinations showed clear lens below age of 45.

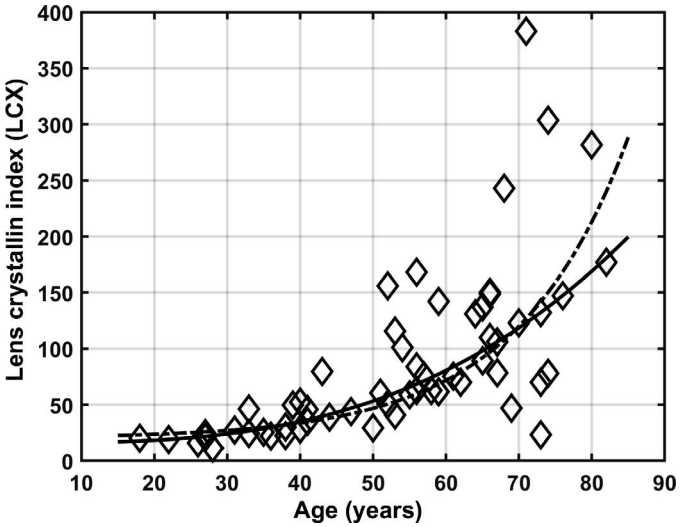

Figure 11. LCX data from site 1 with predicted growth curves. *Solid line* is based on the model for relative lens resistance proposed by Glasser and Campbell,[35] and *dotted line* is a proposed exponential model.

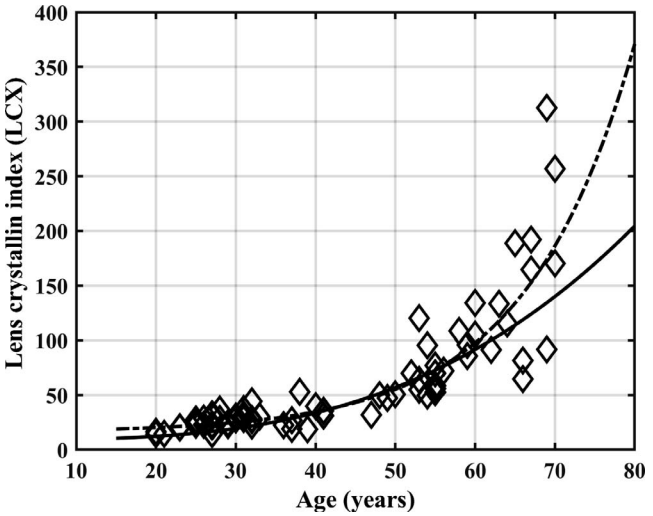

Figure 12. LCX data from site 2 with predicted growth curves. *Solid line* is based on the model for relative lens resistance proposed by Glasser and Campbell,[35] and *dotted line* is a proposed exponential model.

$LCX = 19.9 + \exp(0.066 \times age)$, with an r^2 value of 0.964, and for site 2 is $LCX = 15.9 + \exp(0.074 \times age)$, with an r^2 value of 0.988. Thus, it can be concluded that LCX correlates with an increase in lens rigidity and loss of accommodation.

The reader is reminded that the above results have been obtained across a wide age group and none of the patients were called up for a follow-up measurement. Indeed, the age-related changes correspond to the studied population. However, based on the data, some conclusions can be drawn for any single patient. If longitudinal measurements were possible, a similar trend would likely be observed as a function of age for any one patient. For instance, it is expected that the LCX value will increase with age for all patients; however, the shape of LCX progression is likely to be patient dependent. Thus, for any patient, a few data points taken in the formative years from infancy to age 35 can be used to predict the patient-specific cataract or presbyopia growth curve. Knowledge of such a growth curve is critical for determining the intervention point for administration of therapeutic agents to slow the progression of cataract or presbyopia. Therefore, theoretically with timely intervention, presbyopia and need for cataract surgery can be delayed by many years. However, confirmation of this hypothesis will require the collection of data from the same patient over several decades. In addition, the mentioned spatially localized measurements were made in the nuclear region of the lens. A comprehensive snapshot of the aggregated state of the lens crystallins may be done by performing measurements at several disparate locations in the lens. Future and more advanced designs of the device can include optical coherence tomography to measure the LCX in a specific location, such as center of the nucleus and anterior or posterior subcapsular region. Measurements in a specific location may be more exact for assessing different types of cataract.

Acknowledgments

Disclosures: **A. Abazari**, None; **H.S. Dhadwal**, Integrated Fiber Optic Systems, Inc. (I); **J. Wittpenn**, None

References

1. Flaxman SR, Bourne RRA, Resnikoff S, et al. Global causes of blindness and distance vision impairment 1990–2020: a systematic review and metaanalysis. *Lancet Glob Health*. 2017;5:e1221–e1234.
2. Chua J, Lim B, Fenwick EK, et al. Prevalence, risk factors, and impact of undiagnosed visually significant cataract: the Singapore epidemiology of eye diseases study. *PLoS One*. 2017;12: e0170804.

3. Richter GM, Chung J, Azen SP, Varma R, Los Angeles Latino Eye Study Group. Prevalence of visually significant cataract and factors associated with unmet need for cataract surgery: Los Angeles Latino Eye Study. *Ophthalmology*. 2009;116:2327–2335.
4. Rochtchina E, Mukesh BN, Wang JJ, McCarty CA, Taylor HR, Mitchell P. Projected prevalence of age-related cataract and cataract surgery in Australia for the years 2001 and 2021: pooled data from two population-based surveys. *Clin Exp Ophthalmol*. 2003;31:233–236.
5. Salm M, Belsky D, Sloan FA. Trends in cost of major eye diseases to Medicare, 1991 to 2000. *Am J Ophthalmol*. 2006;142:976–982.
6. Hu TS, Datiles MB, Kinoshita JH. Reversal of galactose cataract with sorbinil in rats. *Invest Ophthalmol Vis Sci*. 1983;24:690–694.
7. Hu TS, Merola L, Kuwabara T, Kinoshita JH. Prevention and reversal of galactose cataracts in rats with topical sorbinil. *Invest Ophthalmol Vis Sci*. 1984;25:603–605.
8. Dhadwal HS, Ansari RR, Dellavecchia MA. Coherent fiber optic sensor for early detection of cataractogenesis in a human eye lens. *Opt Eng*. 1993;32:233–238.
9. Rovati L, Fankhauser F II, Rick J. Design and performance of a new ophthalmic instrument for dynamic light scattering in the human eye. *Rev Sci Instrum*. 1996;66:2615–2620.
10. Ansari RR, Suh KS, Arabshahi A, Wilson WW, Bray TL, DeLucas LJ. A fiber optic probe for monitoring protein aggregation, nucleation and crystallization. *J Cryst Growth*. 1996;168:216–226.
11. Thurston GM, Hayden DL, Burrows P, et al. Light scattering from the aging human lens in vivo. *Curr Eye Res*. 1997;16:197–207.
12. Dhadwal H, Wittpenn J. In vivo dynamic light scattering characterization of the human lens: cataract index. *Curr Eye Res*. 2000;20:502–510.
13. Datiles MB III, Ansari RR, Reed GF. A clinical study of the human lens with a dynamic light scattering device. *Exp Eye Res*. 2002;74:93–102.
14. Ansari RR, Suh KS, Dunker S, Kitaya N, Sebag J. Quantitative molecular characterization of bovine vitreous and lens with non-invasive dynamic light scattering. *Eye Res*. 2001;73:839–866.
15. Datiles MB III, Ansari RR, Suh KI, et al. Clinical detection of precataractous lens protein changes using dynamic light scattering. *Arch Ophhalmol*. 2008;126:1687–1693.
16. Chu B. *Laser Light Scattering—Basic Principles and Practice*. 2nd ed. New York, NY: Academic Press; 1991.
17. Berne BJ, Pecora R. *Dynamic Light Scattering with Applications to Chemistry, Biology and Physics*. New York, NY: John Wiley; 1976.
18. Truscott RJW, Friedrich MG. The etiology of human age-related cataract. Proteins don't last forever. *Biochim Biophys Acta*. 2015;1860:192–198.
19. Grey AC, Schey KL. Age-related changes in the spatial distributions of human lens α–crystallin products by MALDI imaging mass spectroscopy. *Invest Ophthalmol Vis Sci*. 2009;50:4319–4329.
20. Hains PG, Truscott RJW. Age-dependent deamidation of lifelong proteins in the human lens. *Invest Ophthalmol Vis Sci*. 2010;51:3107–3114.
21. Pescosolido N, Barbato A, Giannotti R, Komaiha C, Lenarduzzi F. Age-related changes in the kinetics of human lenses: prevention of the cataract. *Int J Ophthalmol*. 2016;9:1506–1517.
22. Strenk SA, Strenk LM, Koretz JF. The mechanisms of presbyopia. *Prog Retin Eye Res*. 2005;24:379–393.
23. Truscott RJW, Zhu X. Presbyopia and cataract: a question of heat and time. *Prog Retin Eye Res*. 2000;29:487–499.
24. Mohr BG, Dobson CM, Garman SC, Muthukumar M. Electrostatic origin of in vitro aggregation of human γ-crystallin. *J Chem Phys*. 2013;139:121914–121921.
25. *ANSI Z80.36-2016 for Ophthalmics – Light Hazard Protection for Ophthalmic Instruments*. Alexandria, VA: The Accredited Committee Z80 for Ophthalmic Standards, The Vision Council.
26. Satish L, Millan S, Das S, Jena S, Sahoo H. Thermal aggregation of bovine serum albumin in conventional buffers: an insight into molecular level interactions. *J Solution Chem*. 2017;46:831–848.
27. June RK, Cunningham JO, Fyhrie DP. A novel method for curve fitting the stretched exponential function to experimental data. *Biomed Eng Res*. 2013;2:153–158.
28. Muthukumar M. Ordinary-extraordinary transition in dynamics of solutions of charged molecules. *Proc Natl Acad Sci USA*. 2016;113:12627–12632.
29. Frisken BJ. Revisiting the method of cumulants for the analysis of dynamic light-scattering data. *App Opt*. 2001;40:4087–4091.
30. Duane A. Normal values of the accommodation at all ages. *JAMA*. 1912;LIX:1010–1013.

31. Faria-Correia F, Ramos I, Lopez B, Monteiro T, Franqueira N, Ambrosio R Jr. Comparison of dysfunctional lens index and Scheimpflug lens densitometry in the evaluation of age-related nuclear cataracts. *J Refract Surg*. 2016;32:244–248.
32. Faria-Correia F, Ramos I, Lopes B, Monteiro T, Franqueira N, Ambrósio R Jr. Correlations of objective metrics for quantifying dysfunctional lens syndrome with visual acuity and phacodynamics. *J Refract Surg*. 2017;33:79–83.
33. Xu CC, Xue T, Wang QM, Zhou YN, Yu A. Repeatability and reproducibility of a double-pass optical quality analysis device. *PLoS One*. 2015;10:e0117587.
34. Martinez-Roda JA, Vilaseca M, Ondatehui JC, et al. Optical quality and intraocular scattering in a healthy young population. *Clin Exp Optom*. 2011; 94:223–227.
35. Glasser A, Campbell MCW. Biometric, optical and physical changes in the isolated human crystalline lens with age in relation to presbyopia. *Vis Res*. 1999;39:1991–215.